arXiv:1606.04936v2 [cond-mat.supr-con] 27 Feb 2017

Vertical line nodes in the superconducting gap structure of Sr_2RuO_4

E. Hassinger,[1,2,3,*] P. Bourgeois-Hope,[1] H. Taniguchi,[4] S. René de Cotret,[1]
G. Grissonnanche,[1] M. S. Anwar,[4] Y. Maeno,[3,4] N. Doiron-Leyraud,[1] and Louis Taillefer[1,3,†]

[1] *Département de physique & RQMP, Université de Sherbrooke, Sherbrooke, Québec J1K 2R1, Canada*
[2] *Max Planck Institute for Chemical Physics of Solids, 01187 Dresden, Germany*
[3] *Canadian Institute for Advanced Research, Toronto, Ontario M5G 1Z8, Canada*
[4] *Department of Physics, Graduate School of Science, Kyoto University, Kyoto 606-8502, Japan*

(Dated: February 28, 2017)

There is strong experimental evidence that the superconductor Sr_2RuO_4 has a chiral p-wave order parameter. This symmetry does not require that the associated gap has nodes, yet specific heat, ultrasound and thermal conductivity measurements indicate the presence of nodes in the superconducting gap structure of Sr_2RuO_4. Theoretical scenarios have been proposed to account for the existence of deep minima or accidental nodes (minima tuned to zero or below by material parameters) within a p-wave state. Other scenarios propose chiral d-wave and f-wave states, with horizontal and vertical line nodes, respectively. To elucidate the nodal structure of the gap, it is essential to know whether the lines of nodes (or minima) are vertical (parallel to the tetragonal c axis) or horizontal (perpendicular to the c axis). Here, we report thermal conductivity measurements on single crystals of Sr_2RuO_4 down to 50 mK for currents parallel and perpendicular to the c axis. We find that there is substantial quasiparticle transport in the $T = 0$ limit for both current directions. A magnetic field H immediately excites quasiparticles with velocities both in the basal plane and in the c direction. Our data down to $T_c/30$ and down to $H_{c2}/100$ show no evidence that the nodes are in fact deep minima. Relative to the normal state, the thermal conductivity of the superconducting state is found to be very similar for the two current directions, from $H = 0$ to $H = H_{c2}$. These findings show that the gap structure of Sr_2RuO_4 consists of vertical line nodes. This rules out a chiral d-wave state. Given that the c-axis dispersion (warping) of the Fermi surface in Sr_2RuO_4 varies strongly from surface to surface, the small $a - c$ anisotropy suggests that the line nodes are present on all three sheets of the Fermi surface. If imposed by symmetry, vertical line nodes would be inconsistent with a p-wave order parameter for Sr_2RuO_4. To reconcile the gap structure revealed by our data with a p-wave state, a mechanism must be found that produces accidental line nodes in Sr_2RuO_4.

PACS numbers: 74.25.Fy, 74.20.Rp, 74.70.Dd

I. INTRODUCTION

Sr_2RuO_4 is one of the rare materials in which p-wave superconductivity is thought to be realized. Nuclear magnetic resonance [1, 2] and neutron scattering [3] measurements find no drop in the spin susceptibility below the superconducting transition temperature T_c, strong evidence in favour of spin-triplet pairing. Measurements of muon spin rotation [4, 5] and the polar Kerr angle [6] show that time-reversal symmetry is spontaneously broken below T_c. These results (and others) have led to the view that Sr_2RuO_4 has a chiral p-wave order parameter, with a d-vector given by $\mathbf{d} = \Delta_0 \mathbf{z}(k_x \pm ik_y)$ [7–9]. Nevertheless, the symmetry of the superconducting order parameter in Sr_2RuO_4 is still under debate [8, 9]. One of the problems is that although the gap structure of a chiral p-wave order parameter is not required by symmetry to go to zero, *i.e.* to have nodes, anywhere on a two-dimensional Fermi surface, there are in fact low-energy excitations deep inside the superconducting state of Sr_2RuO_4, as detected in the specific heat [10–13], ultrasound attenuation [14] and penetration depth [15] at very low temperature. Theoretical scenarios have been proposed to account for those excitations in terms of either accidental nodes that are perpendicular to the tetragonal c axis (*i.e.* 'horizontal') [16] or deep minima in the superconducting gap along lines parallel to the c axis (*i.e.* 'vertical') [17–20]. The latter vary in depth from sheet to sheet on the three-sheet Fermi surface of Sr_2RuO_4. On the large γ sheet, the gap develops deep minima in the a direction because an odd-parity order parameter must go to zero at the zone boundary.

These scenarios are difficult to reconcile with the specific heat and thermal conductivity of Sr_2RuO_4. When plotted as C_e/T vs T, the electronic specific heat C_e of Sr_2RuO_4 is perfectly linear below $\sim T_c/2$, down to the lowest temperature [10–13]. Gap minima of various depths inevitably lead to deviations from perfect linearity in C_e/T vs T [17]. In the clean limit, a truly linear behaviour can only be obtained if the minima on all three sheets are so deep that they extend to negative values, thereby producing accidental nodes.

The in-plane thermal conductivity $\kappa_a(T)$ of Sr_2RuO_4 decreases smoothly down to the lowest measured temperature, and it extrapolates to a large

*Electronic address: elena.hassinger@cpfs.mpg.de
†Electronic address: louis.taillefer@usherbrooke.ca

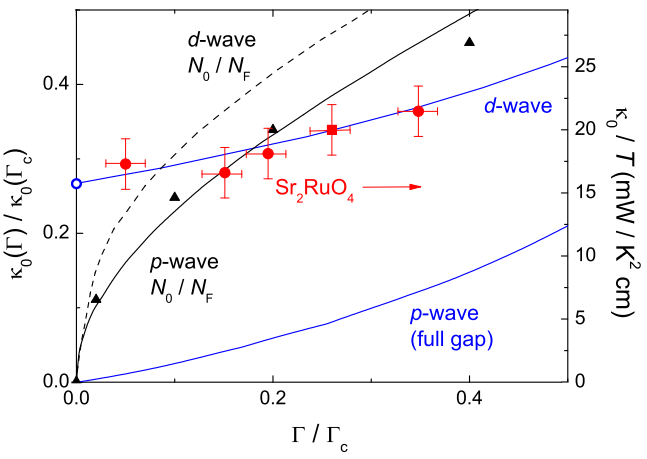

FIG. 1: Residual linear term in the thermal conductivity, κ_0/T, as a function of impurity scattering rate Γ, both normalized to unity at $\Gamma = \Gamma_c$, the critical scattering rate needed to suppress superconductivity. The blue lines are theoretical calculations for a d-wave state [22] and a fully-gapped p-wave state [23], as indicated (left axis). In the clean limit ($\Gamma \to 0$), κ_0/T vanishes in the p-wave case while it reaches a non-zero value in the d-wave case (open circle), whose value is given by Eq. 1, estimated at $\kappa_0/T = 15.8$ mW / K^2 cm in Sr_2RuO_4 (see text). The experimental values of κ_0/T measured in Sr_2RuO_4 are plotted as red symbols (right axis; circles, [21]; square, this work), taking $\hbar\Gamma_c = k_B T_{c0}$. The black lines are the zero-energy density of states N_0, normalized by the normal-state value N_F (left axis; solid, full-gap p-wave [24]; dashed, d-wave [25]). Black triangles show N_0/N_F for a p-wave state with a deep gap minimum ($\Delta_{min} \simeq \Delta_{max}/4$) [26].

residual linear term, κ_0/T, at $T = 0$ [21]. This residual linear term is robust against impurity scattering, and virtually unaffected by a 10-fold increase in scattering rate [21]. This is the classic behaviour of a nodal superconductor whose nodes are imposed by symmetry [22, 25, 27, 28] (Fig. 1), as in the d-wave state of cuprate superconductors [29]. It comes from the linear energy dependence of the density of states at low energy, which produces a compensation between the growth in the density of quasiparticles and the decrease in their mean free path as a function of impurity scattering [27]. Such a compensation does not occur in a nodeless p-wave state [23, 24] (Fig. 1), nor does it occur for accidental nodes in an s-wave state [30].

In summary, the known properties of κ/T and C_e in Sr_2RuO_4 strongly suggest that the low-energy quasiparticles in the superconducting state come from nodes in the gap, not from deep minima. Because accidental nodes do not occur naturally in the chiral p-wave state that is widely proposed for Sr_2RuO_4, it is important to establish the presence of nodes. Moreover, because other proposed states have symmetry-imposed line nodes that are either horizontal (chiral d-wave state [31]) or vertical (f-wave state [32, 33]), we need to determine whether line nodes are vertical or horizontal.

Existing experimental evidence on the direction of line nodes in Sr_2RuO_4 is contradictory. Measurements of the heat capacity as a function of the angle made by a magnetic field H applied in the basal plane (normal to the c axis) relative to the a axis ([100] direction) reveal a small four-fold variation below 0.25 K that is consistent with vertical line nodes along the ΓM directions [12, 13]. However, no such angular variation was detected in the heat conduction down to 0.3 K [34–36]. Moreover, ultrasound attenuation in Sr_2RuO_4 is rather isotropic in the plane, unexpected if line nodes are vertical [14].

In this Letter, we shed new light on the gap structure of Sr_2RuO_4 by using the directional power of thermal conductivity to determine whether the line nodes are vertical or horizontal. In particular, we probe nodal quasiparticle motion along the c axis as $T \to 0$, from measurements of κ_c, the thermal conductivity along the c axis, down to $T_c/30$ (50 mK). We observe a substantial residual term κ_0/T in the c direction at $H = 0$. Moreover, κ_0/T is rapidly enhanced by a magnetic field, even as low as H_{c2} / 100. This confirms that the line nodes in Sr_2RuO_4 are not deep minima and it shows they must be vertical. Furthermore, quantitative analysis suggests that the line nodes are present on all three Fermi surfaces. If the vertical line nodes are imposed by symmetry, then, by virtue of Blount's theorem [37], they would rule out a spin-triplet state, such as the proposed p-wave state [38]. Conversely, if Sr_2RuO_4 is indeed a p-wave superconductor, then a reason must be found for the presence of accidental line nodes in its gap function. Note that the obvious spin-singlet state that breaks time-reversal symmetry has symmetry-imposed line nodes that are horizontal, not vertical [31].

II. METHODS

Single crystals of Sr_2RuO_4 were grown by the floating-zone method [39] and annealed in oxygen flow at 1080 °C for 8 days. Both samples were cut into rectangular platelets from the same crystal rod that contained very few Ru inclusions ($\sim$ 3 inclusions / mm^2). No 3 K anomaly was detected in either the susceptibility of the large annealed crystal or the resistivity of the small measured samples. The a-axis sample had a length of 4.0 mm along the a axis, and a cross-section of 0.3×0.18 mm^2. The c-axis sample had a length of 1.0 mm along the c axis, and a cross-section of 0.4×0.42 mm^2. The geometric factor of the a-axis sample was refined by normalizing the room-temperature resistivity to the well-established literature value of $\rho_a(300\ \mathrm{K}) = 121\ \mu\Omega$ cm [40]. The geometric factor of the c-axis sample was calculated from sample dimensions and contact separation. The value we find is $\rho_c(300\ \mathrm{K}) = 33$ mΩ cm, in the range of reported values [41, 42]. Contacts were made with silver epoxy (Epo-Tek H20E) heated at 450 °C for 1 hour in oxygen flow. Silver wires were then glued on with silver paint. From our thermal conductivity measurements, we obtain

a superconducting transition temperature $T_c = 1.2$ K, consistent with the measured residual resistivity of our a-axis sample, $\rho_{a0} = 0.24\ \mu\Omega$ cm [40]. The thermal conductivity was measured using a one heater-two thermometer method [43], with an applied temperature gradient of 2-5% of the sample temperature. Measurements where carried out for two directions of the magnetic field H: $H \parallel a$ and $H \parallel c$. For $H \parallel a$, the field was aligned to within 1° of the a axis, and perpendicular to the heat current. (For this field direction, a misalignment of 1° can cause a decrease of H_{c2} by 0.1 T [44].) The field was always changed at $T > T_c$.

III. H = 0 : IN-PLANE TRANSPORT

Fig. 2a shows the thermal conductivity of Sr_2RuO_4 in zero field, for the current in the plane ($J \parallel a$). The conductivity κ_a is completely dominated by the electronic contribution [21], κ_e, so that $\kappa_e >> \kappa_p$ up to ~ 3 K, where κ_p is the phonon conductivity. In Fig. 2a, a Fermi-liquid fit to the normal-state data (above T_c) yields $\kappa_N/T = L_0/(a + bT^2)$, where $L_0 \equiv (\pi^2/3)(k_B/e)^2$, with $a = 0.24\ \mu\Omega$ cm and $b = 8$ nΩ cm/K^2. We see that the Wiedemann-Franz law is satisfied, with $a = \rho_{a0}$.

Fig. 2b shows a zoom of the data at low temperature, seen to extrapolate to $\kappa_0/T = 20 \pm 2$ mW/K^{2}cm, a large residual linear term in excellent agreement with the value reported for Sr_2RuO_4 samples of similar T_c [21] (Fig. 1). In the limit of a vanishing impurity scattering rate Γ, whence $T_c \to 1.5$ K, $\kappa_0/T = 17 \pm 2$ mW/K^{2}cm [21]. A ten-fold increase in Γ only yields a modest increase in κ_0/T (Fig. 1). Such a weak dependence of κ_0/T on Γ is precisely the behavior expected of a superconductor with symmetry-imposed line nodes, whereby the impurity-induced growth in the quasiparticle density of states is compensated by a corresponding decrease in mean free path, as in a d-wave superconductor [22, 27, 28] (Fig. 1). (By contrast, accidental nodes and deep minima in an s-wave superconductor are not robust against impurity scattering, so they will in general be lifted or be made shallower, respectively, causing κ_0/T to vanish or decrease with impurity concentration, respectively [30].) In other words, the remarkable fact that κ_0/T remains large [21] even when the zero-energy density of states vanishes [10] as $\Gamma \to 0$ in Sr_2RuO_4 is the clear signature of a line node. Indeed, while impurities in a p-wave superconductor without nodes do induce a zero-energy density of states [23, 24, 26], the associated κ_0/T vanishes as $\Gamma \to 0$ [23, 24] (Fig. 1) because the impurity-induced states are localized.

The magnitude of κ_0/T at $\Gamma \to 0$ can be evaluated theoretically from a knowledge of the Fermi velocity v_F and the gap velocity at the node, v_Δ. For a d-wave gap on a single 2D Fermi surface [28] :

$$\frac{\kappa_0}{T} = \frac{k_B^2}{3\hbar}\frac{1}{c}\left(\frac{v_F}{v_\Delta} + \frac{v_\Delta}{v_F}\right) , \qquad (1)$$

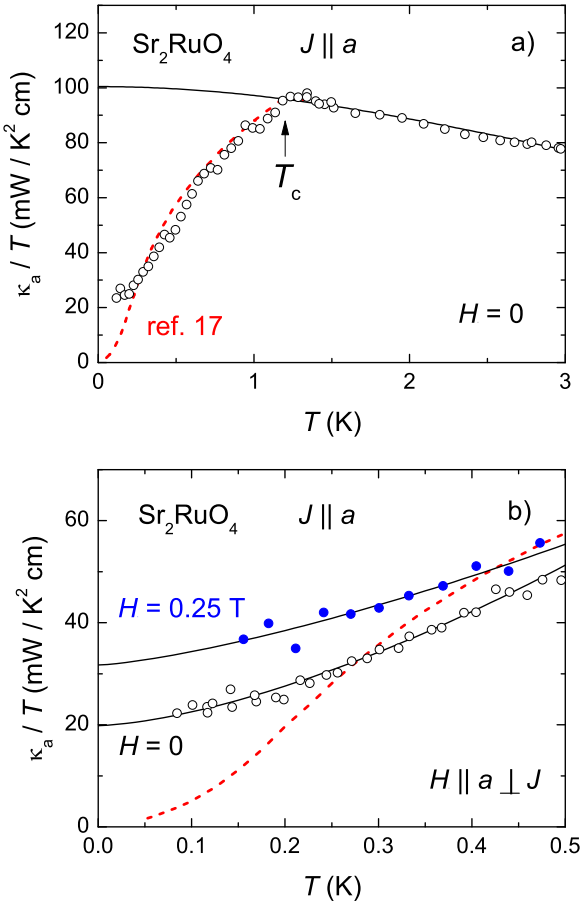

FIG. 2: a) In-plane (a-axis) thermal conductivity $\kappa_a(T)$ of Sr_2RuO_4 at $H = 0$ (open circles). The black line is a Fermi-liquid fit to the normal-state data, $\kappa_N/T = L_0/(a + bT^2)$, extended below T_c. The arrow marks the location of the superconducting transition temperature, $T_c = 1.2$ K, defined as the temperature below which κ/T deviates from its normal-state behavior. Note that the contribution of phonons to κ_a, κ_p, is negligible up to 3 K, so that $\kappa_a \simeq \kappa_e$, the electronic contribution. The red dashed line is a calculation for a three-band model of a p-wave state with deep minima in the gap structure [17] (see text). It provides a good description of the data at high temperature, but it fails below 0.3 K. b) Zoom at low temperature. Data taken in a magnetic field $H = 0.25$ T ($H \parallel a$) are also shown (blue dots). The solid black lines are a fit of the data to the form $\kappa/T = \kappa_0/T + cT^n$.

where c is the interlayer separation along the c axis and $v_\Delta = 2\Delta_0/\hbar k_F$, in terms of the Fermi wavevector k_F and the gap maximum Δ_0, in $\Delta(\phi) = \Delta_0 \cos 2\phi$. This expression works very well for overdoped cuprate superconductors such as $YBa_2Cu_3O_7$ and $Tl_2Ba_2CuO_{6+\delta}$ [45], quasi-2D metals where the pairing symmetry is established to be d-wave. Let us use Eq. 1 to estimate κ_0/T in Sr_2RuO_4.

The Fermi surface of Sr_2RuO_4 is quasi two-dimensional and it has been characterized experimentally in exquisite detail [47]. It consists of three cylinders: two at the center of the Brillouin zone (β and γ) and one (α) at the

corner. The values of k_F and v_F are known precisely for each. In a $d_{x^2-y^2}$-wave state, each cylinder would have four vertical line nodes (along the $x = \pm y$ directions). Assuming the same gap on each Fermi surface and using the weak-coupling expression $\Delta_0 = 2.14\, k_B T_c$, we get $\kappa_0/T = 3.7$, 7.3 and 4.8 mW/K^{2}cm for the α, β and γ sheets, respectively, giving a total conductivity $\kappa_0/T = 15.8$ mW/K^{2}cm (open circle on the y axis of Fig. 1). This theoretical value is in remarkably good agreement with the measured value $\kappa_{a0}/T = 17 \pm 2$ mW/K^{2}cm [21], consistent with line nodes on all three Fermi surfaces.

One may ask whether our data are compatible with deep minima instead of nodes. In Fig. 2, we compare our data with calculations for a model of Sr_2RuO_4 in the clean limit where the gap has symmetry-related minima along the a axis on the γ sheet and very deep minima along the zone diagonals on the α and β sheets, that result from the model interaction [17]. The deepest minima are on the β sheet, where the gap goes down to a value 30 times smaller than its maximal value (on the γ sheet). We see that while the model works well for $T > T_c/4$, it fails at lower T, forced as it is to go to zero at $T \to 0$ since the gap does not have nodes. This comparison shows that our data are inconsistent even with minima so deep that $\Delta_{min} \simeq \Delta_{max}/30$. Taking into account the perfectly linear T dependence of the specific heat below $\sim T_c/2$, the case against deep minima in the gap is compelling, for the combined data require that $\Delta_{min} \simeq \Delta_{max}/100$ on each of the three Fermi surfaces – a rather artificial situation. Note that adding impurities to the calculation by Nomura [17] would produce a non-zero κ_0/T, thereby achieving better agreement with experiment (Fig. 2). However, that magnitude of κ_0/T would be expected to decrease rapidly as $\Gamma_0 \to 0$ [23, 24], contrary to what is observed experimentally [21] (Fig. 1).

IV. H = 0 : C-AXIS TRANSPORT

Fig. 3a shows the conductivity out of the plane, $\kappa_c(T)$ ($J \parallel c$). It is completely dominated by the phonon contribution κ_p, since in this direction κ_e is some 2000 times smaller than in the plane (estimated from the resistivity anisotropy). Because of this, the only way to extract the electronic contribution of interest is to obtain the purely fermionic residual linear term at $T = 0$. A zoom on the c-axis conductivity at low temperature is shown in Figs. 3b and 3c. We see that κ_c/T is linear below 0.2 K. We attribute this linear behavior of κ_p/T, also observed in overdoped cuprate superconductors [52], to the scattering of phonons by nodal quasiparticles, as discussed theoretically in ref. 53.

A linear fit to κ_c/T extrapolates to $\kappa_{c0}/T = 0.0 \pm 3\,\mu$W/K^{2}cm (Fig. 3c). However, $\kappa_c(T)/T$ cannot continue linearly all the way down to $T = 0$, for this would imply a divergent phonon mean free path, since $l_p \propto \kappa/T^3$. The sample boundaries impose an upper bound on l_p. For diffuse (non-specular) scattering, $l_0 = 2\sqrt{S/\pi}$, where S is the sample cross-section normal to the heat flow. In the ballistic regime at low temperature, where phonons are scattered by the (rough) sample boundaries, we have [54]:

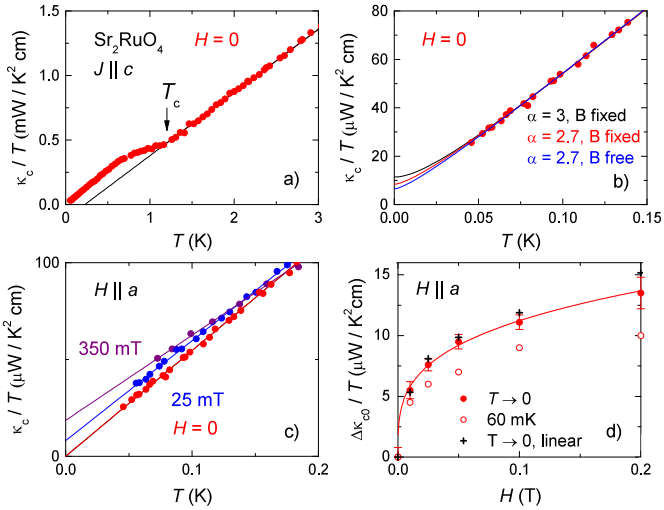

FIG. 3: Out-of-plane (c-axis) thermal conductivity of Sr_2RuO_4. a) At $H = 0$. The black line is a linear fit to the normal-state data. The arrow marks the location of $T_c = 1.2$ K. In this direction, $\kappa_e << \kappa_p$, so that the purely electronic term is obtained as $\kappa_c(T)/T$ in the $T = 0$ limit. b) Zoom on the data at low temperature, at $H = 0$ (red dots). The black line is a fit of the data to Eq. 3 below 0.35 K, with the phonon conductivity in the $T \to 0$ limit given by $\kappa_p = BT^\alpha$, with $\alpha = 3.0$ and B given by sound velocity and sample dimensions (see text). The other two lines are the same fit but with $\alpha = 2.7$, to take into account the effect of specular reflection, and B whether fixed (red line) or free (blue line) (see text). c) Same data as in b) (red, $H = 0$), compared with data in a magnetic field $H = 25$ mT (blue) and $H = 0.35$ T (burgundy), with $H \parallel a$. d) Increase in κ_c/T with field $H \parallel a$, where κ_c/T is either measured at $T = 60$ mK (open circles) or extrapolated to $T = 0$, whether linearly as in panel (c) (crosses) or through a fit as in panel (b), red line (full red dots). The red line is a guide to the eye.

$$\kappa_p = \frac{1}{3} C_p v_p l_0 = BT^3 \quad , \qquad (2)$$

where $C_p = (2\pi^2 k_B/5)(k_B T/\hbar v_p)^3$ is the phonon specific heat [55] and v_p is the average sound velocity. v_p can be extracted from the measured phonon specific heat $C_p/T^3 = 0.197$ mJ/K^4 mole $= 3.44$ J/K^4 m [12], giving $v_p = 3284$ m/s, a value which is consistent with the measured sound velocities in Sr_2RuO_4 [14]. Using Eq. 2, with $l_0 = 0.46$ mm, we get $B = 17.3$ mW / K^4 cm.

The total thermal conductivity is given by $\kappa/T = \kappa_{c0}/T + \kappa_p/T$, where the first term is electronic and the second term is phononic. At low T, two mechanisms scatter phonons: the sample boundaries, already mentioned, and quasiparticles. In Eq. 2, the phonon mean free path l_0 is replaced by $l_p = [1/l_0 + 1/l_e]^{-1}$, where l_e is the

mean free path due to electron-phonon scattering, with $1/l_e \propto T$ [53]. Therefore, in the regime where the latter process dominates, we get $\kappa_p = AT^2$, as seen in our data at $T > 0.05$ K (Fig. 3c). In the limit $T \to 0$, we expect $\kappa_p = BT^3$. We can therefore fit our data to:

$$\kappa/T = \kappa_{c0}/T + BT^2/(1 + BT/A) \quad . \tag{3}$$

Given that B is known and A is fixed by the slope of κ/T above 50 mK, the only free parameter in the fit is the residual linear term κ_{c0}/T, due to quasiparticle transport. A fit to the zero-field data of Fig. 3b yields $\kappa_{c0}/T = 12 \pm 5$ μW / K^2 cm (black line).

Although the cut side surfaces of our c-axis sample are rougher than the mirror-like cleaved or as-grown surface of crystals, there can still be some degree of specular reflection. This was studied on crystals of the cuprate insulator Nd_2CuO_4, with sample surfaces roughened by sanding [54]. At $0.15 < T < 0.3$ K, $\kappa_p = BT^3$, with the prefactor B correctly given by the sound velocities and sample dimensions (Eq. 2). At $T < 0.15$ K, specular reflection becomes important and $\kappa_p = B'T^{2.68}$, with $B' = 0.6B$. Using the same power law to fit our Sr_2RuO_4 c-axis data, namely $\kappa_p = B'T^\alpha$ with $\alpha = 2.7$ and $B' = 0.6$ $B = 10$ μW / K$^{3.7}$ cm, we get the red line in Fig. 3b, with $\kappa_{c0}/T = 8.5$ μW / K^2 cm. Leaving B' as a free fit parameter yields $\kappa_{c0}/T = 6.5$ μW / K^2 cm (blue line). We arrive at a value for the residual linear term of $\kappa_{c0}/T = 10 \pm 5$ μW / K^2 cm.

Nodal quasiparticles in Sr_2RuO_4 must therefore have a non-zero c-axis velocity. This rules out horizontal line nodes – at least in high-symmetry planes (*e.g.* $k_z = 0$) – and it points immediately to vertical line nodes. What magnitude of κ_{c0}/T do we expect if the line nodes responsible for the large in-plane κ_{a0}/T are vertical? Assuming all three Fermi surfaces have line nodes, as would be the case for a $d_{x^2-y^2}$ symmetry, then the a-c anisotropy of nodal quasiparticle transport at $T = 0$, in the superconducting state, should be similar to the a-c anisotropy of transport in the normal state. This is what is observed in the quasi-2D iron-based superconductor KFe_2As_2 [45, 46], for example. Explicitly, $(\kappa_{c0}/T)/(\kappa_{a0}/T) \simeq (\kappa_{cN}/T)/(\kappa_{aN}/T)$, and we therefore expect $\kappa_{c0}/T \simeq 0.2$ $\kappa_{cN}/T = 13 \pm 1\,\mu$W/K^{2}cm, since we have $\kappa_{a0}/T = 0.2$ κ_{aN}/T (Fig. 2) and $\kappa_{cN}/T = 67 \pm 7\,\mu$W/K^{2}cm (see Fig. 4b). This is in good agreement with the experimental value quoted above (10 ± 5 μW / K^2 cm). We conclude that the line nodes in the gap structure of Sr_2RuO_4 are vertical.

In most theoretical proposals, the gap minima do occur along vertical lines. Presumably, some of these minima could accidentally be so deep as to produce nodes. Let us consider different options. First, a scenario of line nodes present only on the α surface is unrealistic because the full contribution of this small surface to the total in-plane conductivity in the normal state is only 18% of κ_{aN}/T [47], less than the zero-field fraction of 20% (Fig. 2b). In other words, the entire α Fermi surface would have to be normal already at $H = 0$. Such an extreme multi-band character is ruled out by two facts: 1) the residual linear term in C_e/T at $T \to 0$ is too small [13]; 2) an increase in impurity scattering does not cause κ_{a0}/T to decrease [21] – unlike in $CeCoIn_5$, where electrons on part of the Fermi surface are uncondensed and $\kappa_{a0}/T \propto 1/\Gamma$ [48].

Secondly, a scenario with nodes only on the β surface is unlikely because the β surface accounts for 80% of the total normal-state conductivity along the c axis, but only 37% along the a axis [47]. As a result, if only the β surface had nodes, it would alone be responsible for the ratio $(\kappa_{a0}/T)/(\kappa_{aN}/T) = 0.2$, and it would then necessarily produce a larger ratio along the c axis (by a factor $\sim 80/37$), giving $(\kappa_{c0}/T)/(\kappa_{cN}/T) \simeq 0.2$ $(80/37) = 0.43$, so that $\kappa_{c0}/T \simeq 29\,\mu$W/K^{2}cm. Such a large value is not possible, since it exceeds the full measured conductivity at $T = 50$ mK (including phonons) (Fig. 3c). Invoking line nodes on both α and β surfaces decreases these estimates to $(\kappa_{c0}/T)/(\kappa_{cN}/T) \simeq 0.2$ $(89/55) = 0.32$ and $\kappa_{c0}/T \simeq 22\,\mu$W/K^{2}cm – still too large.

In summary, quantitative analysis indicates that the vertical line nodes in Sr_2RuO_4 are present on more than one sheet, including the γ sheet (*e.g.* on γ and β), and most likely present on all three sheets of the Fermi surface. This is consistent with the nodal structure of a $d_{x^2-y^2}$ pairing state (with line nodes on all three sheets) and that of a d_{xy} state (with line nodes on γ and β, but not α). The data would also be consistent with a p-wave pairing state with minima on γ and β that are so deep that they extend to negative values and hence produce accidental nodes.

V. FIELD DEPENDENCE

Applying a magnetic field is a sensitive way to probe the low-lying excitations in a type-II superconductor [57]. In the absence of nodes, the quasiparticle states are localized in the vortex cores, and heat conduction proceeds by tunnelling between adjacent vortices, which depends exponentially on inter-vortex separation. As a result, κ_0/T grows exponentially with H, as observed in all s-wave superconductors, *e.g.* LiFeAs [58]. In a two-band s-wave superconductor like $NbSe_2$ [51], the exponential increase is seen below $H^\star << H_{c2}$, the effective critical field of the band with the minimum gap. By contrast, in a nodal superconductor quasiparticle states are delocalized even at $T = 0$ and $H = 0$. Increasing the field immediately increases their density of states, causing the specific heat to increase as $\sqrt{H}$, the so-called Volovik effect. As a result, κ_0/T grows rapidly with H at the lowest fields [59], as observed in d-wave superconductors, *e.g.* $YBa_2Cu_3O_y$ [60].

In Fig. 3c, we show c-axis data at $H = 25$ mT. We see that even this tiny field ($H_{c2}/50$) induces a substantial increase in κ_c/T at $T \to 0$. This proves the existence of nodal quasiparticles with c-axis velocity. In Fig. 3d, a plot of κ_c/T vs H shows how rapid the rise is, whether

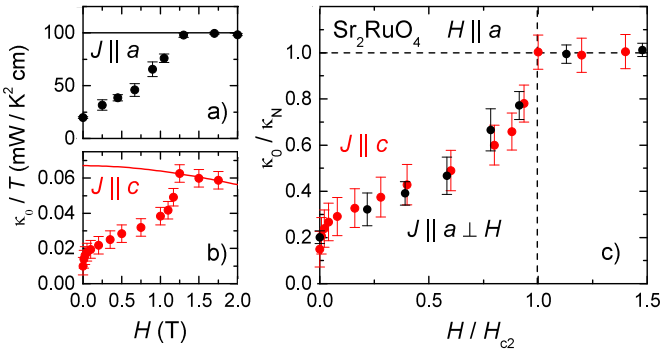

FIG. 4: Residual linear term κ_0/T as a function of a magnetic field H applied along the a axis ($H \parallel a$). a) For a current in the plane ($J \parallel a$). The data points (black dots) are κ_{a0}/T obtained by fitting κ_a/T *vs* T as in Fig. 1b. The black line is a constant fit to the data above H_{c2} (negligible magnetoresistance for that current direction). It defines κ_{aN}/T *vs* H, and it is consistent with the $H = 0$ value obtained by extrapolating κ_N/T above T_c to $T \to 0$ (Fig. 2a). b) Same as in a), but for a current along the c axis ($J \parallel c$). The data points (red dots) are κ_{c0}/T obtained by fitting κ_c/T *vs* T as in Fig. 3b. Above H_{c2}, κ_{c0}/T decreases slightly due to magnetoresistance (see text). The red line is a fit of the data above H_{c2} to $\kappa_N/T = a/(b + cH^2)$, which defines κ_{cN}/T *vs* H for this current direction. The value at $H \to 0$ is $\kappa_{cN}/T = 67 \pm 7\,\mu$W/K^{2}cm. c) Field dependence of κ_{a0}/T (black dots) and κ_{c0}/T (red dots) normalized to their normal-state value, both plotted as $(\kappa_0/T)/(\kappa_N/T)$ *vs* H/H_{c2}, with $H_{c2} = 1.25$ T. For simplicity, we define $\kappa_0/\kappa_N \equiv (\kappa_0/T)/(\kappa_N/T)$. The error bars on κ_0/κ_N come from the combined uncertainties in extrapolating κ/T to $T = 0$ to obtain κ_0/T and in extending κ_N/T below H_{c2}.

κ_c/T is measured at $T = 60$ mK (open circles) or extrapolated to $T = 0$, either linearly as in Fig. 3c (crosses) or through the fit described in sec. IV (full red circles).

In Fig. 4, we show the H dependence of κ_0/T in Sr_2RuO_4 ($H \parallel a$), for both current directions. Both κ_{a0}/T and κ_{c0}/T have the dependence expected of nodal superconductors, as calculated for a single-band d-wave superconductor [59].

In Fig. 4c, we compare the H dependence of κ_{a0}/T and κ_{c0}/T in normalized units, both plotted as $(\kappa_0/T)/(\kappa_N/T) \equiv \kappa_0/\kappa_N$ *vs* H/H_{c2}. We obtain the normal-state conductivity κ_N/T below H_{c2} by extending a fit of the data above H_{c2} to lower fields. For $J \parallel a$, there is negligible H dependence up to 4 T, and so we take κ_N/T to be constant (Fig. 4a). For $J \parallel c$, Sr_2RuO_4 exhibits a sizable magneto-resistance, which varies as H^2 below 2 T or so [61]. By the Wiedemann-Franz law, this implies that $\kappa_N/T = a/(b+cH^2)$. A fit of the data above H_{c2} to this formula yields the red line in Fig. 4b.

The data in Fig. 4c are striking: the two normalized curves are the same, at all fields, within error bars. This is strong confirmation that line nodes are vertical. Indeed, horizontal line nodes would inevitably produce a qualitative difference between the two current directions,

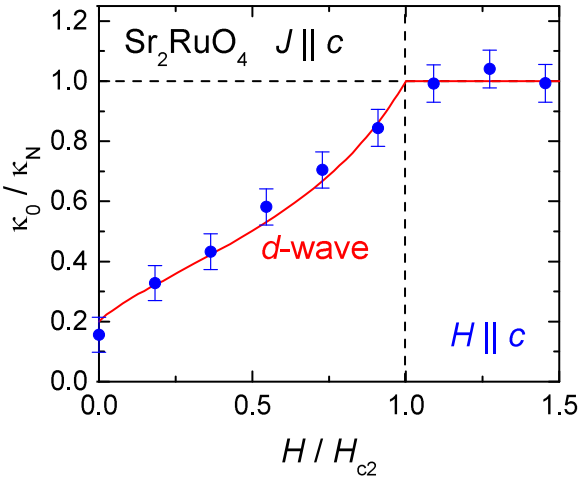

FIG. 5: Residual linear term κ_0/T as a function of magnetic field, for a field along the c axis ($H \parallel c$) and a heat current along the c axis ($J \parallel c$). The data are plotted as $(\kappa_0/T)/(\kappa_N/T)$ *vs* H/H_{c2}, with $H_{c2} = 0.055$ T. For this field direction (in the longitudinal configuration with a tiny H_{c2}), the magneto-resistance in the normal state is negligible, and so κ_N/T is a constant below H_{c2}. The data points are κ_{c0}/T obtained by fitting κ_c/T *vs* T as in Fig. 3b (red fit). The solid red line is a theoretical calculation for a single-band d-wave superconductor [63].

roughly d-wave-like (rapid) for κ_{a0}/T and s-wave-like (exponential) for κ_{c0}/T. The fact that both curves in Fig. 4c are the same is also consistent with line nodes being present on all of the three Fermi surfaces. Indeed, if line nodes were present only on the β surface, for example, κ_{c0}/T would exhibit a d-wave-like H dependence, as it is dominated by that surface, while κ_{a0}/T would exhibit an s-wave-like H dependence, since it is dominated by the other Fermi surfaces.

The electronic specific heat at low temperature also displays a rapid increase at low field. In the $T = 0$ limit, the residual linear term $\gamma_0(H)$ reaches $\sim 30\%$ of its normal-state value γ_N by $H \simeq 0.1\ H_{c2}$ ($H \parallel a$), and then increases more slowly at higher H [11, 13]. We see from Fig. 4c, that the field dependences of κ_0/κ_N and γ_0/γ_N are similar. To explain the rapid initial rise in γ_0/γ_N *vs* H, it was proposed that the α and β surfaces become normal at a field $H^\star \simeq 0.1\ H_{c2}$ [12]. But this is inconsistent with our data, since it would imply a much larger increase in κ_0/κ_N for $J \parallel c$ than for $J \parallel a$, given that the β surface accounts for 80% of κ_{cN}/T but only 37% of κ_{aN}/T. This is not observed (Fig. 4c).

In Fig. 5, we show the effect of applying a magnetic field parallel to the c axis. This is the field direction for which the Volovik effect is the dominant excitation process, and for which most theoretical calculations on quasi-2D superconductors have been carried out (*e.g.* [59]). The overall field dependence of κ_0/κ_N is in good agreement with calculations for a single-band 2D d-wave superconductor [63], as seen in Fig. 5. Also, the specific

heat of Sr_2RuO_4 exhibits a nice $\sqrt{H}$ dependence and detailed $\sqrt{H}/T$ scaling [13], consistent with the behavior of a single-band d-wave superconductor [62].

VI. SUMMARY

In summary, our thermal conductivity measurements confirm that the gap structure of Sr_2RuO_4 has nodes rather than deep gap minima and they reveal that those nodes are vertical lines along the c axis.

In a nutshell, everything about the thermal conductivity of Sr_2RuO_4 is consistent with a d-wave pairing state, including its absolute magnitude at $T \to 0$, its dependence on temperature, magnetic field and impurity scattering, and its isotropy relative to current direction. A d-wave gap structure is also consistent with the specific heat of Sr_2RuO_4 [10–13], including the magnitude of its jump at T_c and its dependence on temperature, magnetic field and impurity scattering.

Given that calculations find p-wave and d-wave solutions for Sr_2RuO_4 to be very close in energy [64], it is tempting to consider a d-wave state for Sr_2RuO_4. However, this comes into conflict with some important properties of the material, in particular the absence of a drop in the NMR Knight shift below T_c [1, 2], a signature of spin-triplet pairing, and the onset of muon and Kerr signals below T_c [4, 6], evidence that time-reversal symmetry is broken. These are the natural properties of a chiral p-wave superconductor. Note that the spin-singlet chiral d-wave state also breaks time-reversal symmetry, but its gap function varies as $k_z(k_x + ik_y)$ and therefore has symmetry-imposed line nodes that are horizontal, not vertical [31].

We are therefore faced with a situation where Sr_2RuO_4 appears to adopt a p-wave state with a d-wave-like gap structure. An intriguing solution to this conundrum has been proposed in the so-called f-wave state [32, 33], a combination of B_g and E_u representations ($B_g \times E_u$), where B_g is either B_{1g} ($d_{x^2-y^2}$) or B_{2g} (d_{xy}), with gap functions that vary either as $(k_x^2 - k_y^2)(k_x + ik_y)$ or as $(k_x k_y)(k_x + ik_y)$, respectively.

Further theoretical and experimental work is needed to resolve the puzzle presented to us by the superconducting state of this exceptionally well characterized and otherwise rather conventional three-band metal.

VII. ACKNOWLEDGEMENTS

We thank J. Corbin, S. Fortier, A. Juneau-Fecteau, and F. F. Tafti for their assistance with the experiments, and A. Balatsky, M. Graf, A. P. Mackenzie, K. Samokhin, M. Sato, J. Sauls, T. Scaffidi, R. Thomale, and S. Yonezawa for stimulating discussions. L.T. acknowledges support from the Canadian Institute for Advanced Research (CIFAR) and funding from the National Science and Engineering Research Council of Canada (NSERC), the Fonds de recherche du Québec - Nature et Technologies (FRQNT), the Canada Foundation for Innovation (CFI) and a Canada Research Chair. The work in Japan was supported by the JSPS KAKENHI (No. JP15H05852).

[1] K. Ishida, H. Mukuda, Y. Kitaoka, K. Asayama, Z. Q. Mao, Y. Mori, and Y. Maeno, *Spin-triplet Superconductivity in Sr_2RuO_4 identified by ^{17}O Knight shift*, Nature **396**, 658 (1998).

[2] K. Ishida, M. Manago, T. Yamanaka, H. Fukazawa, Z. Q. Mao, Y. Maeno, and K. Miyake, *Spin polarization enhanced by spin-triplet pairing in Sr_2RuO_4 probed by NMR*, Phys. Rev. B **92**, 100502 (2015).

[3] J. A. Duffy, S. M. Hayden, Y. Maeno, Z. Mao, J. Kulda, and G J. McIntyre, *Polarized-Neutron Scattering Study of the Cooper-Pair Moment in Sr_2RuO_4*, Phys. Rev. Lett. **85**, 5412 (2000).

[4] G. M. Luke *et al.*, *Time-reversal symmetry-breaking superconductivity in Sr_2RuO_4*, Nature **394**, 558 (1998).

[5] G. M. Luke *et al.*, *Unconventional superconductivity in Sr_2RuO_4*, Physica B **289**, 373 (2000).

[6] J. Xia, Y Maeno, P. T. Beyersdorf, M. M. Fejer, and A. Kapitulnik, *High resolution polar Kerr effect measurements of Sr_2RuO_4: Evidence for broken time-reversal symmetry in the superconducting state*, Phys. Rev. Lett. **97**, 167002 (2006).

[7] A. P. Mackenzie, and Y. Maeno, *The superconductivity of Sr_2RuO_4 and the physics of spin-triplet pairing*, Rev. Mod. Phys. **75**, 657 (2003).

[8] Y. Maeno, S. Kittaka, T. Nomura, S. Yonezawa, and K. Ishida, *Evaluation of Spin-Triplet Superconductivity in Sr_2RuO_4*, J. Phys. Soc. Jap. **81**, 011009 (2012).

[9] C. Kallin, *Chiral p-wave order in Sr_2RuO_4*, Rep. Prog. Phys. **75**, 042501 (2012).

[10] S. Nishizaki, Y. Maeno, and Z. Mao, *Effect of impurities on the specific heat of the spin-triplet superconductor Sr_2RuO_4*, J. Low Temp. Phys. **117**, 1581 (1999).

[11] S. Nishizaki, Y. Maeno, and Z. Mao, *Changes in the Superconducting State of Sr_2RuO_4 under Magnetic Fields Probed by Specific Heat*, J. Phys. Soc. Japan **69**, 572 (2000).

[12] K. Deguchi, Z. Q. Mao, H. Yaguchi, and Y. Maeno, *Gap Structure of the Spin-Triplet Superconductor Sr_2RuO_4 Determined from the Field-Orientation Dependence of the Specific Heat*, Phys. Rev. Lett. **92**, 047002 (2004).

[13] K. Deguchi, Z.Q. Mao and Y. Maeno, *Determination of the Superconducting Gap Structure in All Bands of the Spin-Triplet Superconductor Sr_2RuO_4*, J. Phys. Soc. Japan **73**, 1313 (2004).

[14] C. Lupien, W. A. MacFarlane, C. Proust, L. Taillefer, Z. Q. Mao and Y. Maeno, *Ultrasound Attenuation in Sr_2RuO_4: An Angle-Resolved Study of the Superconduct-*

ing Gap Function, Phys. Rev. Lett. **86**, 265986 (2001).
[15] I. Bonalde, B. D. Yanoff, M. B. Salamon, D. J. Van Harlingen, E. M. E. Chia, Z. Q. Mao, and Y. Maeno, *Temperature Dependence of the Penetration Depth in Sr_2RuO_4: Evidence for Nodes in the Gap Function*, Phys. Rev. Lett. **85**, 4775 (2000).
[16] M. E. Zhitomirsky and T. M. Rice, *Interband Proximity Effect and Nodes of Superconducting Gap in Sr_2RuO_4*, Phys. Rev. Lett. **87**, 057001 (2001).
[17] T. Nomura, *Theory of Transport Properties in the p-Wave Superconducting State of Sr_2RuO_4A Microscopic Determination of the Gap Structure*, J. Phys. Soc. Japan **74**, 1818 (2005).
[18] S. Raghu, A. Kapitulnik, and S. A. Kivelson, *Hidden Quasi-One-Dimensional Superconductivity in Sr_2RuO_4*, Phys. Rev. Lett. **105**, 136401 (2010).
[19] Q. H. Wang, C. Platt, Y. Yang, C. Honerkamp, F. C. Zhang, W. Hanke, T. M. Rice, and R. Thomale, *Theory of superconductivity in a three-orbital model of Sr_2RuO_4*, Europhys. Lett. **104**, 17013 (2013).
[20] T. Scaffidi, J. C. Romers, and S. Simon, *Pairing symmetry and dominant band in Sr_2RuO_4*, Phys. Rev. B **89**, 220510 (2014).
[21] M. Suzuki, M. A. Tanatar, N. Kikugawa, Z. Q. Mao, Y. Maeno, and T. Ishiguro, *Universal Heat Transport in Sr_2RuO_4*, Phys. Rev. Lett. **88**, 227004 (2002).
[22] Y. Sun and K. Maki, *Transport properties of d-wave superconductors with impurities*, Europhys. Lett. **32**, 355 (1995).
[23] K. Maki and E. Puchkaryov, *Impurity scattering in isotropic p-wave superconductors*, Europhys. Lett. **45**, 263 (1999).
[24] K. Maki and E. Puchkaryov, *Impurity effects in p-wave superconductors*, Europhys. Lett. **50**, 533 (2000).
[25] Y. Sun and K. Maki, *Impurity effects in d-wave superconductors*, Phys. Rev. B **51**, 6059 (1995).
[26] K. Miyake and O. Narikiyo, *Model for Unconventional Superconductivity of Sr_2RuO_4: Effect of Impurity Scattering on Time-Reversal Breaking Triplet Pairing with a Tiny Gap*, Phys. Rev. Lett. **83**, 1423 (1999).
[27] M. J. Graf, S-K. Yip, J. A. Sauls, and D. Rainer, *Electronic thermal conductivity and the Wiedemann-Franz law for unconventional superconductors*, Phys. Rev. Lett. **53**, 15147 (1996).
[28] A. C. Durst and P.A. Lee, *Impurity-induced quasiparticle transport and universal-limit Wiedemann-Franz violation in d-wave superconductors*, Phys. Rev. B **62**, 1270 (2000).
[29] L. Taillefer, B. Lussier, R. Gagnon, K. Behnia, and H. Aubin, *Universal heat conduction in $YBa_2Cu_3O_{6.9}$*, Phys. Rev. Lett. **79**, 483 (1997).
[30] V. Mishra, A. Vorontsov, P. J. Hirschfeld, and I. Vekhter, *Theory of thermal conductivity in extended-s state superconductors: Application to ferropnictides*, Phys. Rev. B **80**, 224525 (2009).
[31] I. Zutic and I. Mazin, *Phase-Sensitive Tests of the Pairing State Symmetry in Sr_2RuO_4*, Phys. Rev. Lett. **95**, 217004 (2005).
[32] Y. Hasegawa, M. Machida and K. Ozaki, *Spin-Triplet Superconductivity with Line Nodes in Sr_2RuO_4*, J. Phys. Soc. Japan **69**, 336 (2000).
[33] M. J. Graf and A. Balatsky, *Identifying the pairing symmetry in the Sr_2RuO_4 superconductor*, Phys. Rev. B **62**, 9697 (2000).
[34] K. Izawa, H. Takahashi, H. Yamaguchi, Yuji Matsuda, M. Suzuki, T. Sasaki, T. Fukase, Y. Yoshida, R. Settai, and Y. Onuki, *Superconducting Gap Structure of Spin-Triplet Superconductor Sr_2RuO_4 Studied by Thermal Conductivity*, Phys. Rev. Lett. **86**, 2653 (2001).
[35] M. Tanatar, M. Suzuki, S. Nagai, Z. Q. Mao, Y. Maeno, and T. Ishiguro, *Anisotropy of Magnetothermal Conductivity in Sr_2RuO_4*, Phys. Rev. Lett. **86**, 2649 (2001).
[36] M. Tanatar, M. Suzuki, S. Nagai, Z. Q. Mao, Y. Maeno, and T. Ishiguro, *Thermal conductivity of superconducting Sr_2RuO_4 in oriented magnetic fields*, Phys. Rev. B **63**, 064505 (2001).
[37] E. I. Blount, *Symmetry properties of triplet superconductors*, Phys. Rev. B **32**, 2935 (1985).
[38] S. Kobayashi, K. Shiozaki, Y. Tanaka, M. Sato, *Topological Blounts theorem of odd-parity superconductors*, Phys. Rev. B. **90**, 024516 (2014).
[39] Z. Q. Mao, Y. Maeno, H. Fukuzawa, *Crystal growth of Sr_2RuO_4*, Mater. Res. Bull. **35**, 1813-1824 (2000).
[40] A. P. Mackenzie, R. K. W. Haselwimmer, A. W. Tyler, G. G. Lonzarich, Y. Mori, S. Nishizaki, and Y. Maeno, *Extremely Strong Dependence of Superconductivity on Disorder in Sr_2RuO_4*, Phys. Rev. Lett. **80**, 161 (1998).
[41] A. W. Tyler, A. P. Mackenzie, S. Nishizaki, and Y. Maeno, *High-temperature resistivity of Sr_2RuO_4: Bad metallic transport in a good metal*, Phys. Rev. B **58**, 10107 (1998).
[42] Y. Maeno, H. Hashimoto, K. Yoshida, S. Nishizaki, T. Fujita, J. G. Bednorz, F. Lichtenberg, *Superconductivity in a layered perovskite without copper*, Nature **372**, 32 (1994).
[43] J.-Ph. Reid, M. A. Tanatar, X. G. Luo, H. Shakeripour, N. Doiron-Leyraud, Ni Ni, S. L. Bud'ko, P. Canfield, R. Prozorov, L. Taillefer, *Nodes in the gap structure of the iron arsenide superconductor $Ba(Fe_{(1-x)}Co_x)_2As_2$ from c-axis heat transport measurements*, Phys. Rev. B **82**, 064501 (2010).
[44] S. Kittaka, T. Nakamura, Y. Aono, S. Yonezawa, K. Ishida, and Y. Maeno, *Angular dependence of the upper critical field of Sr_2RuO_4*, Phys. Rev. B **80**, 174514 (2009).
[45] J.-Ph. Reid *et al.*, *From d-wave to s-wave pairing in the iron-pnictide superconductor (Ba, K)Fe_2As_2*, Supercond. Sci. Technol. **25**, 084013 (2012).
[46] J.-Ph. Reid *et al.*, *Universal heat conduction in the iron-arsenide superconductor KFe_2As_2 : Evidence of a d-wave state*, Phys. Rev. Lett. **109**, 087001 (2012).
[47] C. Bergemann, A. P. Mackenzie, S. R. Julian, D. Forsythe, and E. Ohmichi, *Quasi-two-dimensional Fermi liquid properties of the unconventional superconductor Sr_2RuO_4*, Adv. Phys. **52**, 639 (2003).
[48] M. A. Tanatar *et al.*, *Unpaired electrons in the heavy-fermion superconductor $CeCoIn_5$*, Phys. Rev. Lett. **95**, 067002 (2005).
[49] F. Bouquet, R. A. Fisher, N. E. Phillips, D. G. Hinks, and J. D. Jorgensen, *Specific heat of (MgB_2)-B-11: Evidence for a second energy gap*, Phys. Rev. Lett. **87**, 047001 (2001).
[50] A.V. Sologubenko, J. Jun, S. M. Kazakov, J. Karpinski, and H. R. Ott, *Thermal conductivity of single-crystalline MgB_2*, Phys. Rev. B **66**, 014504 (2002).
[51] E. Boaknin *et al.*, *Heat conduction in the vortex state of $NbSe_2$: Evidence for multiband superconductivity*, Phys. Rev. Lett. **90**, 117003 (2003).
[52] D. G. Hawthorn *et al.*, *Doping dependence of the su-*

perconducting gap in $Tl_2Ba_2CuO_{6+}$ from heat transport, Phys. Rev. B **75**, 104518 (2007).

[53] M.F. Smith, *Low-T phononic thermal conductivity in superconductors with line nodes*, Phys. Rev. B **72**, 052511 (2005).

[54] S. Y. Li, J.-B. Bonnemaison, A. Payeur, P. Fournier, C. H. Wang, X. H. Chen, and L. Taillefer, *Low-temperature phonon thermal conductivity of single-crystalline Nd_2CuO_4: Effects of sample size and surface roughness*, Phys. Rev. B **77**, 134501 (2008).

[55] N. W. Ashcroft and N. D. Mermin, 1976, *Solid State Physics*, (Philadelphia: Sounders College Publishing)

[56] M. Sutherland *et al.*, *Thermal conductivity across the phase diagram of cuprates: Low-energy quasiparticles and doping dependence of the superconducting gap*, Phys. Rev. B **67**, 174520 (2003).

[57] H. Shakeripour, C. Petrovic, L. Taillefer, *Heat transport as a probe of superconducting gap structure*, New J. Phys. **11**, 055065 (2009).

[58] M. A. Tanatar *et al.*, *Isotropic three-dimensional gap in the iron arsenide superconductor LiFeAs from directional heat transport measurements*, Phys. Rev. B **84**, 054507 (2011).

[59] I. Vekhter and A. Houghton, *Quasiparticle Thermal Conductivity in the Vortex State of High- T_c Cuprates*, Phys. Rev. Lett. **83**, 4626 (1999).

[60] M. Chiao, R. W. Hill, C. Lupien, B. Popic, R. Gagnon, and L. Taillefer, *Quasiparticle Transport in the Vortex State of $YBa_2Cu_3O_{6.9}$*, Phys. Rev. Lett. **82**, 2943 (1999).

[61] N. E. Hussey *et al.*, *Normal-state magneto-resistance of Sr_2RuO_4*, Phys. Rev. B **57**, 5505 (1998).

[62] S. H. Simon and P. A. Lee, *Scaling of the Quasiparticle Spectrum for d-wave Superconductors*, Phys. Rev. Lett. **78**, 1548 (1997).

[63] H. Kusunose, T. M. Rice and M. Sigrist, *Electronic thermal conductivity of multigap superconductors: Application to MgB_2*, Phys. Rev. B **66**, 214503 (2002).

[64] A. Steppke *et al.*, *Strong peak in T_c of Sr_2RuO_4 under uniaxial pressure*, Science **355**, 148 (2017).